

Utilization of multiple quantity sensors for estimation of characteristics of internal combustion engine

Abstract: In this paper method of estimation of combustion engine power and torque based on road test is shown. In this particular test the measurement is performed using three axial accelerometer and rate gyroscope fastened to car's chassis. Estimation of main engine characteristics is made with use of measured quantities such as: car mass and acceleration collected in function of vehicle linear velocity. The most essential problems in this approach, considered as primary method errors, are minimization of underestimation of moment of inertia of rotating elements in drivetrain and efficiency of drivetrain itself. Moreover it is vital to determine as precise as possible vehicle acceleration and its linear velocity in presence of disturbances – mainly chassis movements and additional accelerations, which comes from pavement unevenness (roughness). In this article application of several sensors of different quantities for increase of accuracy of PAAF II (Power Acceleration And Force) device in relation to prototype device predecessor is taken into consideration. Results of utilization of measurements data and calculation algorithms specific for both devices were compared in aspects of estimation of engine power as well as torque..

Key words: write engine power, torque, estimation, road test, 3-axial accelerometer.

Zastosowanie sensorów wielu wielkości do estymacji charakterystyk silnika spalinowego

Streszczenie: W pracy przedstawiono metodę estymacji przebiegów momentu i mocy silnika w oparciu o test drogowy, w którym bezpośredni pomiar wykonywany jest z użyciem trzyosiowego akcelerometru i żyroskopu zamocowanych do nadwozia samochodu. Estymacja podstawowych charakterystyk silnika realizowana jest w oparciu o zmierzone masę pojazdu i przyspieszenie w funkcji jego prędkości liniowej. Podstawowymi problemami w tym podejściu, które uznawane są za podstawowe błędy metody, są minimalizacja niedoszacowania masowego momentu bezwładności elementów wirujących oraz sprawności układu przeniesienia napędu. Ponadto istotne jest także jak najdokładniejsze określenie przyspieszenia i prędkości liniowej pojazdu w obecności zakłóceń - głównie ruchów nadwozia i dodatkowych przyspieszeń pochodzących od nierówności drogi. W tej pracy omówiono zastosowanie czujników wielu wielkości do zwiększenia dokładności urządzenia PAAF II (Power Acceleration And Force) w odniesieniu do urządzenia prototypowego. Porównano wyniki estymacji przebiegu mocy, siły napędowej i momentu dokonanych za pomocą pomiarów i algorytmów obliczeniowych właściwych dla obu urządzeń.

Słowa kluczowe: moc silnika, moment, estymacja, test drogowy, akcelerometr trzyosiowy.

1. Introduction

Since eight years in Opole University of Technology the PAAF prototype device is used for powertrain testing. PAAF utilizes acceleration signal as input in road test. In such testing the car acceleration and mass are used for calculation of driving force and power. Inertial methods are considered as less accurate and even less reliable than the other ones. This is because of many variables, which affecting the measurement, and which influence was eliminated or reduced in dynamometers methods. Specifically they are: wind speed, humidity, temperature, road induced rolling resistance, suspension stiffness and mass distribution, road roughness potholes and bumps [1,4,5].

Since the powertrain parameters estimation is recently intensive explored then it can be stated that

the engine parameters estimation i.e. power and torque is the most challenging task with use of such method. The issue lies in factors, which direct and indirect influence the powertrain parameters measurement and also the engine parameters itself. They can be listed as follows:

1. Unknown or partially known moments of inertia of all rotating elements during test.
2. Drivetrain efficiency which reduces the calculated engine power and torque in relation to measured powertrain's driving force and power.
3. Vehicle velocity trend, which affects engine rotational speed calculation, even if gear ratio is precisely known.
4. Tire slip, which reduces vehicle acceleration during test and distorts engine's rotational speed value

5. Grade resistance change during test, which affect the vehicle driving force value as well as measured acceleration due to both gravity and longitudinal accelerations projections on measurement axes.
6. Vehicle chassis movement during test. Mainly the pitching up during accelerating and pitching down during deceleration, and also rolling caused by road roughness. These movements affecting the measured acceleration by causing projections of measured longitudinal acceleration on measurement axes and also entering unwanted accelerations.

This analysis is a starting point in effort to make inertial methods more accurate. So, the investigation should head into four main directions, which are:

- grade resistance compensation,
- road disturbances filtration,
- pitch angle compensation,
- velocity trend reduction or elimination,

because only thru measurement algorithm improvements a progress can be made in making this device more suitable for main engine characteristics estimation.

2. Research

This investigations aim is to research the possibility of PAAF measurement algorithm improvement in order to estimate the engine power and torque on the basis of road test with use of multi-sensor approach. Particularly the purpose was to find method for pitch angle and compensation for reduce longitudinal acceleration signal distortions caused by chassis movement and local road grade resistance changes during road test (estimated only in deceleration phase).

2.1 Objects of investigations

Two vehicles were used: first with "soft" suspension and the other with "medium/hard" one. The first was Citroën C5, equipped with SI V6 3l engine and automatic power transmission, which was switched into manual mode. CAN BUS is utilized for data exchange between gearbox and engine ECUs and it was used as data source in measurement. The second car was Seat EXEO with 2.0l turbocharged petrol engine and with manual 6 gear gearbox [2,3,6].

2.2 Measurement devices

The measurement system consists of four main parts: combined sensor which is Microstrain's 3DM-GX3-25, SYS-TEC USB-CAN modul-1 interface, National Instruments NI USB 621x M series DAQ card and ELM323 OBD2/RS232 converter (fig. 1).

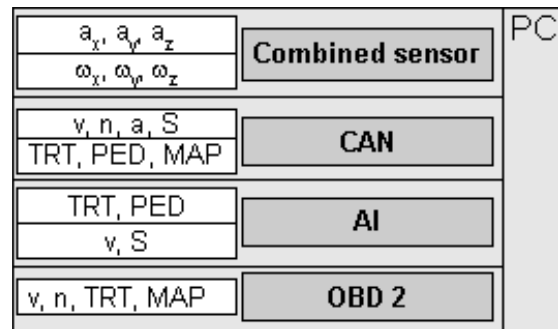


Fig. 1. Measurement system schema [3]

Acquired data are processed by special developed LabView (fig. 2) application running on Windows XP on PC with CELERON 1.6 GHz and 1MB RAM.

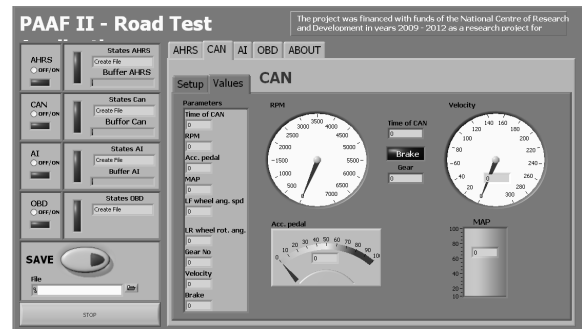


Fig. 2. Window of developed CAR.vi application [6]

This application allows, besides CAN and OBD data acquisition, receiving information thru analog to digital converter specifically for Corrsys L350 measurement head – for precision distance and linear velocity measurement [6].

2.3 Investigations course

For determining the car's acceleration as well as powertrain driving force and power special road test has been developed, which speed profile is shown in figure 3.

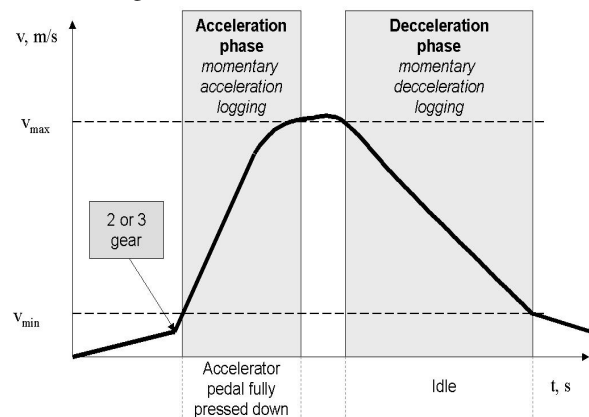


Fig. 3. Velocity profile of road test

All of the road tests were performed on 2nd gear. In first phase car has to accelerate with highest intensity from v_{min} velocity to v_{max} . During this phase the longitudinal acceleration a_l of the car and

other quantities (ref. figure 1) are measured. The a_i value is relative to driving force. Furthermore driving force changes depends on engine characteristics and total car mass. The second phase occurs after the maximum velocity is reached. Then, with decoupled transmission, deceleration is realized. It is assumed that the measured acceleration is negative and depends only on the total movement resistance [1,4]. The test results were stored on mass memory. Further they can be used as input to Matlab in order to perform additional processing and analysis [2,3,6].

2.4 Evaluation of driving force and power

The results from only the first, acceleration phase (powertrain power and driving force) can be interpreted only as gross values [4]. It is so because the results achieved through this method are reduced by movement resistances. In summary, it can be stated that calculated driving force F_{dr} and power with the use of only one phase road test can be different for two the same cars but equipped with other tires or with chassis modifications [1].

$$F_{dr} - F_r - F_a - F_i = 0 \quad (1)$$

For calculation of power and driving force of the power train the formula (1) is utilized, which describes the force balance with inertial force with inertial force F_i included.

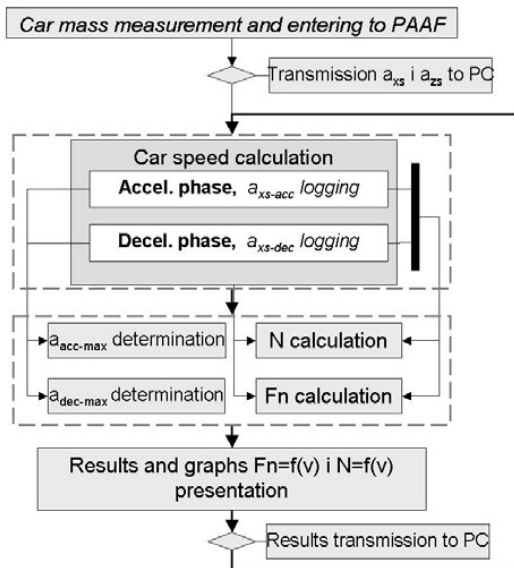


Figure 4. Main algorithm used for calculation powertrain power and driving force

It is obvious that the main resistance values or they totals must be familiar (rolling force and F_r , aerodynamic force F_a or their total value).

It can be achieved in a particularly designed road test, where beside car acceleration phase, additional deceleration values will be acquired while car is decelerating without coupled power transmission as shown on main algorithm schematic on figure 4.

3. Algorithms

There were several road test data calculation algorithms investigate in order to find out which offers the best performance and repeatability. In all cases the source is the rough algorithm described in section 2.3 and discussed in the following one, which is native for both PAAF and PAAF II prototypes.

1st algorithm

With initial pitch angle compensation. It utilizes only data from one of accelerometer axis, which were aligned as close as possible to direction parallel to car's movement. In this case the initial pitch angle α_{p0} was no greater than $\pm 3^\circ$. Compensation of α_{p0} was done by using simple averaging over time equal to 3s.

2nd algorithm

Both - dynamic and initial pitch angle compensation. The algorithm in first stage is the same as the 1st, but after compensation of the initial pitch angle the dynamic pitch angle α_{pd} is calculated as a integral of ω_p and incorporated in further calculations.

3rd algorithm

With all sensors axes rotation in order to align xy axes parallel to horizontal plane and all sensors x axes fixation in movement direction. The algorithm utilizes data from all axes of accelerometer to perform calculate sensor's related coordinate system rotation. After that the z axis should be parallel to gravity vector. The direction vector is determined by calculating of angle of acceleration vector in horizontal plane when car increases speed and then the a_{xs} axes is aligned to it by performing another rotation.

4th algorithm

The algorithm in first stage is the same as the 3rd, but after axes aligning process the pitch angle is compensated by only comparing estimated with measured velocity.

4. Results

The results presented below are the trials of estimation of power and driving force for selected car, which was performed according road test course described in section 2.3 but with use of different algorithms.

4.1 Acceleration and velocity estimation

Utilization of such simple algorithm described above leads to many inaccuracies as mentioned in [4].

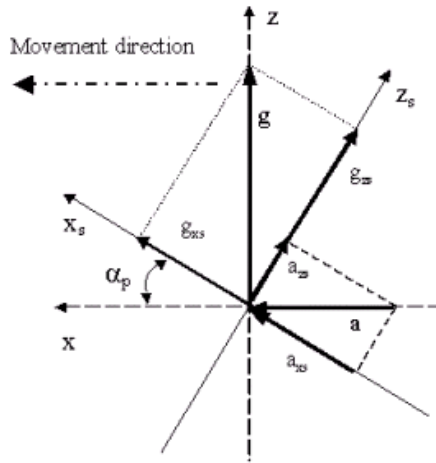


Figure 5. Orientation of car's coordinate system (x_s , z_s) in relation to global (x , z) one when pitch angle α_p value is other than zero [1]

The most important are the lack of compensation of pitch angle, misaligning of main measurement axis in horizontal plane, and additive acceleration created by projection of earth acceleration on main measurement axis. They happens during acceleration and deceleration phases and is caused by reorientation of measurement coordinate system in relation to assumed global coordinate system relative to earth acceleration and movement direction [1,8], as shown on figure 5.

Acceleration projection on measurement axis causes two effects: speed underestimation and so known velocity trend, which is slow build up of velocity value calculated as integral of acceleration. Velocity build up is uncoupled with real one and is caused mainly by sensor's own and road induced noises. This phenomenon can be seen on figure 6, where at end of test the estimated velocity was over 16 m/s, higher then the real one. Such velocity profiles were observed for both 1st and 3rd algorithms, but for 3rd the maximum value was higher.

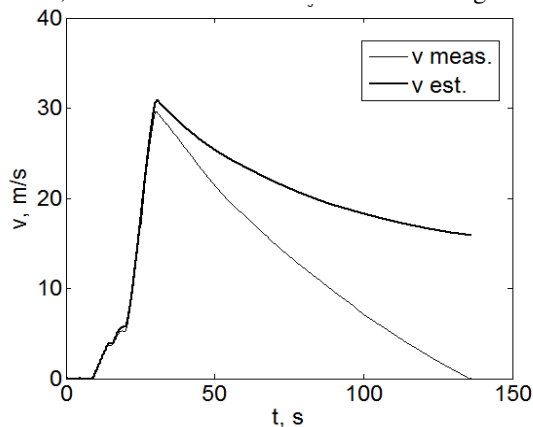


Fig. 6. Comparison of measured and estimated velocity obtained using 1st algorithm for second car

Applying integrated over time gyroscope output (estimation of pitch angle change) for a_1 accelera-

tion correction improves velocity estimation accuracy (fig. 7). But in these tests with such equipment it was limited up to 120s and was strongly influenced by movement induced ω disturbances, which distribution is other than normal.

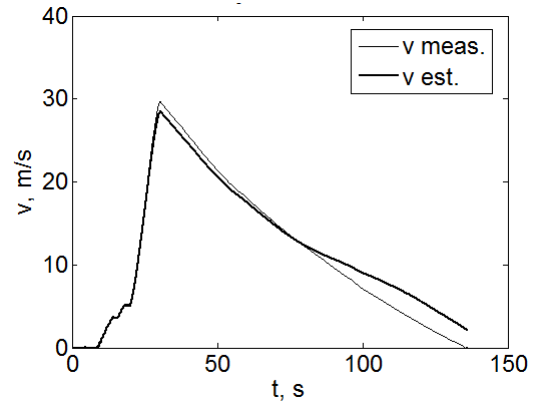


Fig. 7. Comparison of measured and estimated velocity profile calculated using 2nd algorithm for second car

In these test the estimated velocity diverges from real one from $t=90s$ and the final velocity difference was $v_{est}=2.3m/s$.

4th algorithm utilizes frequently comparing of actual and estimated velocity in order to estimate dynamic pitch angle. If there is a difference between these two velocities then it is assumed that it is caused by pitch angle change and additional acceleration is added to longitudinal acceleration to compensate α_{pd} influence. It results in good estimation of velocity profile as can be seen on figure 8. The velocity difference at end of test was the lowest values in whole investigation and was equal only to 0.74 m/s.

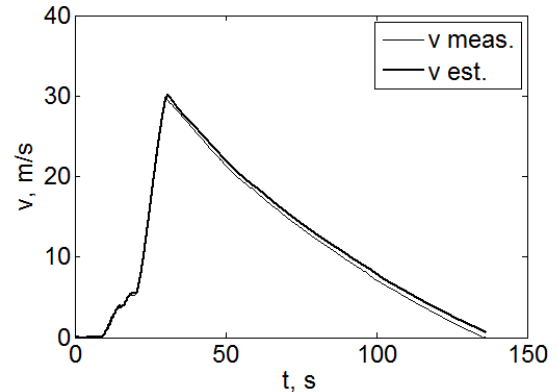


Fig. 8. Comparison of measured and estimated velocity profile calculated using 4th algorithm for second car

4.2 Power and driving force estimation

Utilization of first and third algorithm leads to similar effects. As shown on figure 7 the shape of driving force and power curves are regular, typical for turbocharged petrol engines [9]. The highest estimated power values were $N_{max}=140.91kW$ and

141.50 kW respectively. The driving force highest values were $F_{drmax} = 6.05$ kN and $F_{drmax} = 6.51$ kN accordingly. These algorithms gave very similar results to first modification one. The maximum values are slightly grater $N_{max}=141.50$, $F_{drmax}=6.54$ kN probably because of elimination of horizontal misalign of acceleration sensor.

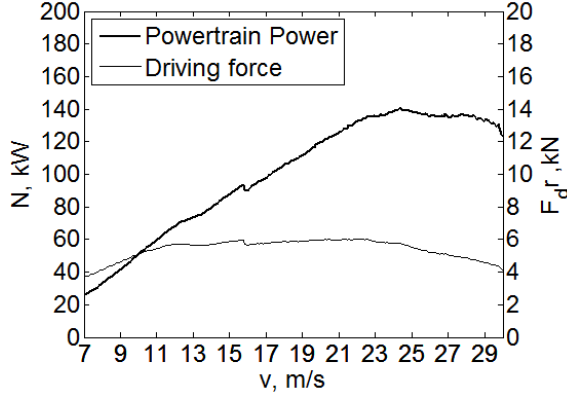


Fig. 9. Powertrain power and driving force curves estimated for second car with use of 1st algorithm

Velocity difference was no greater than 0.2 m/s and its profile were very similar to that one in first case. Similarly like in first one errors in power estimation in free deceleration phase were observed (5% to 15). For these algorithms (1 and 3) flat and horizontal test way is needed and stiff suspension for minimization dynamic pitch angle changes.

In second algorithm dynamic pitch angle α_p estimation is used to correct acceleration values. The angle is calculated as ω_p integral. As can be seeing on figure 9 the N and F_{dr} curves are similar to those in earlier case, but the highest values are smaller and equal to $N_{max}=124.10$ kW and $F_{drmax}=5.80$ kN.

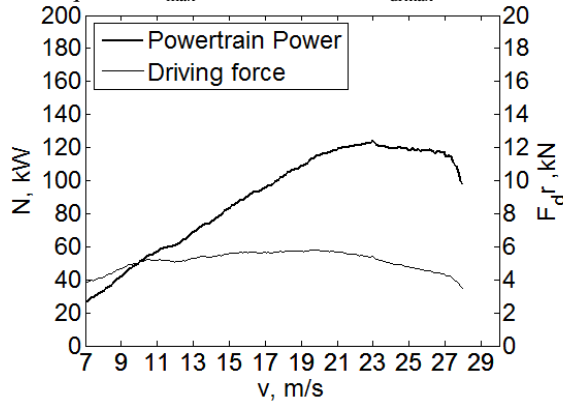


Fig. 10. Powertrain power and driving force curves estimated for second car with use of 2nd algorithm

The power values are about 16kW lower than in first main algorithm modification. This is because of underestimated velocity on top of velocity profile about 2m/s (compare figures 9 ad 10) even if its, which is clearly visible on figure 10. At the end of test the difference between measured and estimated velocity was $v_{est}=2.3$ m/s.

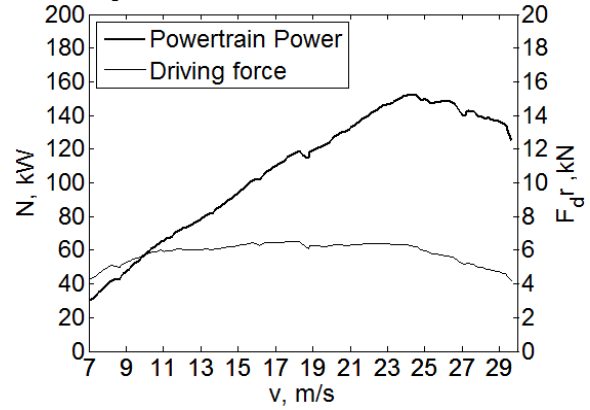


Figure 11. Powertrain power and driving force curves estimated second car with use of 4th algorithm

4th algorithm gave overestimated power and driving force values Maximum estimated powertrain power was equal to ($N_{max}=152.50$ kW) and driving force ($F_{drmax} = 6.51$ kN). Curves shapes (fig. 11) were different for maximum velocities over N_{max} . In this range it was decreasing linear and in other cases the diminishing was more “polynomial”.

5. Conclusion

The results of application of PAAFII prototype algorithm modifications are collected in table 1.

Table 1. Main algorithm modifications performance

Main algorithm modification performance			
	Description	N, kW	F_{dr} , kN
1	Initial pitch angle compensation.	140.90	6.05
2	Dynamic and initial pitch angle compensation.	124.10	5.80
3	Sensors axes rotation to horizontal plane and all sensors x axes fixation in movement direction	141.50	6.54
4	The algorithm in first stage is the same as the 3 rd , but after aligning the pitch angle is compensated by comparing estimated with measured velocity	152.50	6.51

First and third algorithm output is nearly the same because of comparable sensor to the driving direction. In the second - the output is lower because of velocity and pitch angle trend.

The fourth modification output is 7 kW higher than the engine power declared by producer (145kW). Power measured by this method should be from 5% to 15% less than the engine power because of less than unity drivetrain efficiency and tire slip during acceleration. The highest values, even when velocity compensation method were applied, are due to use of velocity from CAN bus. The real one can be different because of inflation pressure, uneven tires load, temperature and rotational speed. When velocity data from optical sensor were utilized the power were $N_{max} = 132.60$ kW, $F_{drmax} = 5.97$ kW which lay in ten percent range of assumed acceptable method error.

MEMS (Micro-Electro-Mechanical System) angular rate sensor is very useful in short term pitch compensation (up to 100s – 120s). Such sensor should be used rather during rapid acceleration for pitch angle compensation or for magnetic sensor dynamic calibration.

Velocity input signal for 4th implementation of measurement algorithm should be received from

device which describes the chassis speed rather than from wheels rotational speed dependent sources. The preferred inputs are GPS (Global Positioning System) or external optical sensor like Corrsys L350.

Velocity calculated from wheel rotational speed is affected by many factors such as dynamic radius change, tires inflation unevenness and change, road profile and velocity dependent disturbances with complex spectral characteristics and therefore it significantly reduces the compensation property of 4th algorithm.

Moreover, the rotational speed represents the wheel behavior, and can be significantly higher during acceleration with high values of driving force than velocity obtained from GPS because of well known tire slip phenomena [5,9].

Acknowledgements

The hereby scientific study was financed with funds of the National Centre for Research and Development in years 2009 – 2012 as a research project for number N R10 0059 06.

Nomenclature/Skróty i oznaczenia

α	angle / kąt,	a_{zs}	acceleration measured on accelerometer z_s axis in m/s^2 / przyspieszenie mierzone w kierunku osi z sensora,
α_p	pitch angle in rad or deg / kąt pochylenia wzdłużnego,	a_z	real longitudinal acceleration in m/s^2 / przyspieszenie w kierunku osi z ,
α_{p0}	initial pitch angle in rad or deg / początkowy kąt pochylenia wzdłużnego,	F_a	aerodynamic force in N / siła oporu aerodynamicznego,
α_{pd}	dynamic pitch angle in rad or deg / dynamiczny kąt pochylenia wzdłużnego,	a_{zs}	acceleration measured on accelerometer z_s axis in m/s^2 / przyspieszenie mierzone w kierunku osi z sensora,
$a_{acc-max}$	maximal measured longitudinal acceleration in car acceleration phase in m/s^2 / największe zmierzone przyspieszenie wzdłużne podczas fazy rozbiegu,	F_{dr}	driving force in N / siła napędowa,
$a_{dec-max}$	maximal measured longitudinal deceleration in car deceleration phase in m/s^2 / największe zmierzone przyspieszenie wzdłużne podczas fazy wybiegu,	F_{drmax}	highest driving force value in test in N / największa wartość siły napędowej w teście
a_l	longitudinal acceleration in m/s^2 / przyspieszenie wzdłużne,	F_i	inertial force in N / siła bezwładności,
a_x	real longitudinal acceleration in m/s^2 / przyspieszenie w kierunku osi x ,	F_r	rolling resistance force in N / siła oporu tocznienia,
a_{xs}	acceleration measured on accelerometer x_s axis in m/s^2 / przyspieszenie mierzone w kierunku osi x sensora,	g	earth acceleration $9.81 m/s^2$ / przyspieszenie ziemskie,
a_{xs-acc}	momentary deceleration in acceleration phase measured on x_s axis in m/s^2 / chwilowe przyspieszenie wzdłużne podczas fazy rozbiegu,	N	power in kW / moc,
a_{xs-dec}	momentary acceleration in acceleration phase measured on x_s axis in m/s^2 / chwilowe przyspieszenie wzdłużne podczas fazy wybiegu,	N_{max}	highest power value in test in kW / największa wartość mocy w teście,
		t	time in s / czas,
		v	linear velocity, car speed in m/s / prędkość pojazdu,
		v_{est}	estimated velocity, m/s / szacowana prędkość pojazdu,
		v_{min}	road test initial velocity in m/s / początkowa prędkość podczas testu drogowego,
		v_{max}	road test final velocity in m/s / końcowa prędkość podczas testu drogowego,

x	global longitudinal axis / <i>oznaczenie globalnej osi wzdłużnej</i> ,	z_s	sensor related vertical measurement axis / <i>oznaczenie osi pionowej sensora</i> ,
x_s	sensor related longitudinal measurement axis/ <i>oznaczenie osi wzdłużnej sensora</i> ,	PAAF	Power Acceleration And Force – abbreviation of device and device prototype name / <i>nazwa prototypu Moc Przyspieszenie i Siła</i>
z	global vertical axis / <i>oznaczenie osi pionowej</i> ,		

Bibliography/Literatura

- [1] S. Brol, J. Mamala, J. Jantos. Assessment of passenger car driveability with use of two axis accelerometer mounted on car body. *Journal of Ultragarsas*, Vol. 59, No 2, Vilno, 2006.
- [2] S. Brol, J. Mamala, J. Jantos. Development of PAAF II device for road vehicles testing. W: 11th International Workshop on research and education in mechatronic Ostrava, Czech Republic 09-10.09, 2010.
- [3] S. Brol, J. Mamala, J. Jantos. Estimation of engine power during road test. W: International Congress Motor Vehicles & Motors 2010 "Sustainable development of automotive industry" Kragujevac, Serbia 07-09.10, 2010. s. 25.
- [4] J. Jantos, S. Brol, J. Mamala. Problems in assessing road vehicle drivability parameters determined with the aid of accelerometer. *SAE Transactions, JOURNAL OF PASSENGER CAR: MECHANICAL SYSTEMS*, Vol. 116, paper no 2007-01-1473, pp. 1318-1324, USA, 2008.
- [5] J. Mamala, S. Brol, J. Jantos. Estimation of the characteristics of powertrain on the basis of measurement of car acceleration, *Studia i Monografie*, vol. 235, Oficyna Wydawnicza Politechniki Opolskiej, Opole, 2008.
- [6] J. Mamala, S. Brol, J. Jantos, J. Korniak. Diagnostics of the drivetrain in a passenger car. W: 10th International Symposium on Advanced Vehicle Control. Loughborough 22-26.08, 2010. s. 508-513.
- [7] J. Merkisz, S. Mazurek, J. Pielecha. *Pokładowe urządzenia rejestrujące w samochodach*. Wydawnictwo Politechniki Poznańskiej, 2007.
- [8] J. Reimpell, J. Betzler. *Podwozia samochodów - Podstawy konstrukcji*. WKŁ Warszawa 2004.
- [9] W. Siłka. *Teoria ruchu samochodu*. WNT Warszawa, 2002.

Mr Sebastian Brol, DEng. – Assistant Professor of Mechanical Engineering at Opole University of Technology.

Dr inż. Sebastian Brol – adiunkt na Wydziale Mechanicznym Politechniki Opolskiej.



Mr Jerzy Jantos, DSc, DEng. – Professor in the Faculty of Mechanical Engineering at Opole University of Technology.

Dr hab. inż. Jerzy Jantos, Prof. PO – profesor na Wydziale Mechanicznym Politechniki Opolskiej.



Mr Jarosław Mamala, DEng. – Assistant Professor in the Faculty of Mechanical Engineering at Opole University of Technology.

Dr inż. Jarosław Mamala – adiunkt na Wydziale Mechanicznym Politechniki Opolskiej.

